

Asymmetric Transfer Hydrogenation of Ketones Using New Iron(II) (P-NH-N-P') Catalysts: Changing the Steric and Electronic Properties at Phosphorus P'

Samantha A. M. Smith,^[a] Demyan E. Prokopchuk,^[a] and Robert H. Morris^{*,[a]}

Abstract: The asymmetric transfer hydrogenation (ATH) of ketones is an efficient method for producing enantio-enriched alcohols which are used as intermediates in a variety of industrial processes. Here we report the synthesis of new iron ATH precatalysts (*S,S*)-[FeBr(CO)(Ph₂PCH₂CH₂NHCHPhCHPhNC=CHCH₂PR'₂)] [BPh₄] (R' = Et, and *ortho*-tolyl (*o*-Tol)) where one of the phosphine groups is modified with small alkyl and large aryl substituents to probe the effect of this change on the activity and selectivity of the catalytic system. A simple reversible equilibrium kinetic model is used to obtain the initial TOF and the inherent enantioselectivity $S = k_r/k_s$ of these catalysts along with those for the previously reported catalysts with R' = Ph and Cy for the ATH of acetophenone. With an increase in the size of the PR'₂ group, the TOF goes through a maximum at PPh₂ while the *S* value

goes through a maximum of 510 at R' = Cy. The complex with R' = *o*-Tol starts with a high *S* value of 200 but is rapidly changed to a second catalyst with an *S* value of 28. For the reduction of acetophenone to (*R*)-1-phenylethanol, turnover numbers of up to 5200 and ee up to 98% were achieved. The chemotherapeutic pharmaceutical precursor (*R*)-(3',5'-bis(trifluoromethyl))-1-phenylethanol is synthesized in up to 95% ee. Several other alcohols can be prepared in greater than 90% ee by choosing the precatalyst with the correctly matched steric properties. A hydride complex derived from the catalyst with R' = Cy is characterized by NMR spectroscopy. It is proposed that low concentration *trans*-hydride carbonyl complexes with the FeH parallel to the NH of the ligand are the active catalysts in all of these systems.

Keywords: homogeneous catalysis · iron catalysis · asymmetric transfer hydrogenation

1. Introduction

The asymmetric reduction of ketones is a challenging process that is useful for many industries including pharmaceutical and fine chemical. Usually precious-metal-based catalysts are employed.^[1] The use of abundant metals such as iron for this transformation is attractive due to their lower cost and toxicity, and this has been a topic of much interest in the last decade.^[2] Recently discovered iron catalysts stand out for their high enantioselectivity and activity in the asymmetric transfer hydrogenation of ketones.^[2b,c,m,3]

The activity and selectivity of our iron-based ATH catalysts (Figure 1) has steadily improved using the reduction of acetophenone by isopropanol as a test case. Our first generation ATH precatalyst (*R,R*)-**A** in isopropanol produced, after activation by isopropoxide, (*S*)-1-phenylethanol in 63% ee (TOF 400, TON 1630 h⁻¹ at 24 °C)^[2h,4] although this ATH system likely involves iron nanoparticles.^[5] Kinetic and mechanistic studies uncovered a high energy barrier for the activation of our more active second generation ATH precatalysts **B** that involved the reduction of one of the imine groups of the **B**.^[2i,1,3a] Our group conducted a stereo-electronic study of complexes **B** that involved varying the substituents R of the phosphine moieties of the P-N-N-P ligand and found that only the use of aryl groups led to very active catalysts for the ATH of ketones.^[6] It was unclear from these studies

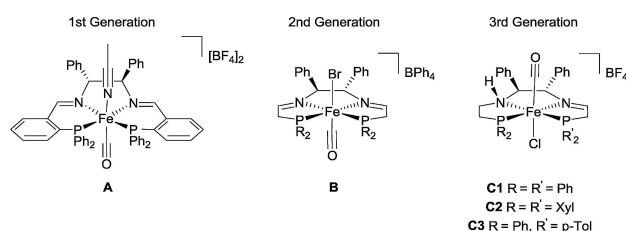


Figure 1. Three generations of ATH Precatalysts.

whether some of the complexes with R = alkyl were inactive due to a high energy barrier to the reduction of the imine of the ligand that is needed for activation or due to a higher barrier for catalysis after imine reduction. The work described below helps to answer this question.

The design of the third generation precatalysts **C** (Figure 1) eliminates this activation barrier by providing the amine-imine ligand structure. This dramatically increases the

[a] S. A. M. Smith, D. E. Prokopchuk, R. H. Morris
Department of Chemistry, University of Toronto, 80 Saint George St. Toronto, Ont. Canada M5S 3H6
E-mail: rmmorris@chem.utoronto.ca

Supporting information for this article is available on the WWW under <https://doi.org/10.1002/ijch.201700019>

ATH activity of the catalyst systems in basic isopropanol when aryl groups are on the phosphine donors. The ATH of acetophenone catalyzed by **C1** ($R=R'=Ph$) produces (*R*)-1-phenylethanol in 78% ee (*R*) with a turnover number (TON) of 5000 and turnover frequency (TOF) $100,000\text{ h}^{-1}$ at 28°C while that by **C2** gives 90% ee (*R*).^[3b] The use of other aryl ketones yielded alcohols with ee greater than 90% (*R*) in certain cases.^[3b,7] The initial work showed that a complex could be prepared with phosphorus donors with different groups on each side, namely **C3** with $R=Ph$, $R'=4\text{-MeC}_6\text{H}_3$. The **C3** system reduced acetophenone with comparable activity to **C1** but with lower enantioselectivity, 70% ee (*R*).^[3b]

Complex **C4** with $R=Ph$ and $R'=Cy$ (Figure 2) was found to be more stereoselective but much less active for ketone reduction than **C1-C3**.^[3c] For example the **C4** system catalyzed the reduction of acetophenone to (*R*)-1-phenylethanol in 98% ee.^[3c] The complex was assumed to have a *trans* configuration shown on the left of Figure 2. Recently, **C4** was crystallized and was found to adopt an unexpected *cis-β* geometry (Figure 2, right).^[8] An objective of the current work is to investigate whether this *cis-β* geometry is of relevance to the activity and selectivity of **C4** relative to **C1**.

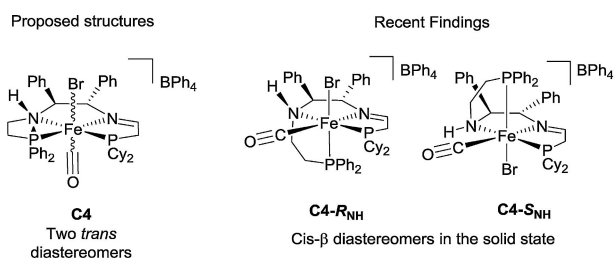


Figure 2. Previously proposed and recently discovered geometries of **C4** with a *cis-β* stereochemistry

Herein, we introduce two other PR'_2 substituents into the Fe(II) complexes *trans*-[FeBr(CO)(PPh₂-NH-N-PR'₂)]⁺, the small, basic PEt₂ donor and the large, less basic P(*o*-Tol)₂ donor while keeping the PPh₂ group constant. This work explores a wider range of stereochemical and electronic properties in order to better understand the relationship between the structures and the resulting activity and enantioselectivity of the catalysts for the reduction of a variety of ketone structures. Simulating the reaction progress of the reductions also sheds light on the factors that determine how quickly the ee of the product alcohol is lost after the reaction reaches equilibrium. We also investigate the properties of the active hydride-containing species.

2. Results and Discussion

2.1 Preparation and Characterization of Complexes

The syntheses of the new iron(II) precatalysts were carried out using routes developed in our lab previously.^[3b,6b,9] Complexes (*S,S*)-**1** with $R'=Et$ and (*S,S*)-**2** with $R'=o\text{-Tol}$ were synthesized using the enantiopure (*S,S*)-PPh₂CH₂CH₂NHCHPhCHPhNH₂ compound and the phosphonium dimers **D1** or **D2**,^[10] respectively, in two main steps (Scheme 1).

First an intermediate complex is made *in situ* by the reaction of the appropriate phosphonium dimer with base, Fe(II), and an enantiopure (*S,S*)-PNN ligand in acetonitrile. On the basis of previous work^[3b,6b,9] this is assumed to be a *trans-bis*(acetonitrile) complex. This is then treated with 1 atm CO and excess KBr. The complexes (*S,S*)-**1** and (*S,S*)-**2** were precipitated as the BPh₄⁻ salts in 35 and 56% yield, respectively, with respect to the starting (*S,S*)-P-NH-NH₂ compound. Complex (*S,S*)-**1** was produced as a mixture of two *trans* diastereomers with structures **E** and **E'** (Figure 3) with ³¹P{¹H} NMR properties very similar to **C1** and **C4** in



Samantha Smith studied Honours Chemistry and Mathematics as a double major at Wilfrid Laurier University where she was first exposed to research. She continued on to the University of Toronto's Department of Chemistry where she is currently working on a Ph. D.

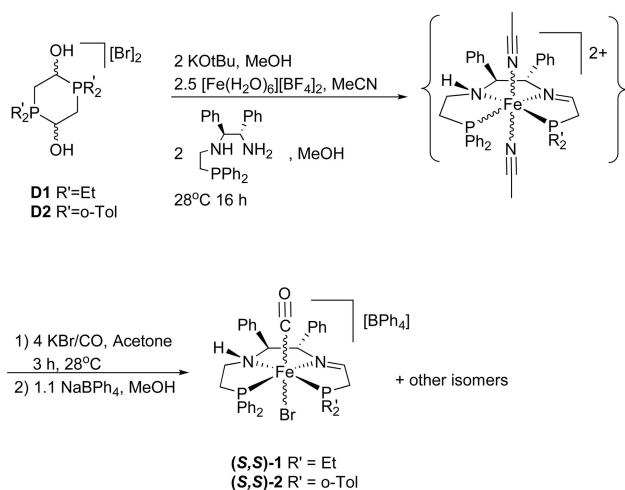


Demyan Prokopchuk was born in Saskatoon, Canada. He received his undergraduate degree from the University of Saskatchewan in 2009 and his PhD from the University of Toronto in 2015 under the supervision of Prof. Robert Morris. He is currently a postdoctoral fellow at Pacific Northwest National Laboratory in the Center for Molecular Electrocatalysis, directed by R. Morris Bullock. His current research interests include ligand design and electro-



chemistry for applications in small molecule activation.

Bob Morris is a professor of chemistry at the University of Toronto. He was born in Ottawa in 1952. He received his PhD from the University of British Columbia in 1978. After postdoctoral work at the Nitrogen Fixation Laboratory, University of Sussex and the Pennsylvania State University he joined the faculty of the University of Toronto in 1980. He was appointed full Professor there in 1989 and served as Acting Chair and Chair of the Chemistry Department from 2008–2013. His research interests include inorganic, organic and catalytic chemistry with applications in the fine chemical industry. He is a Fellow of the Royal Society of Canada and of the Chemical Institute of Canada and a Killam Research Fellow (2015-2017).



Scheme 1. The two-step synthesis of complexes (**S,S**)-1 and (**S,S**)-2

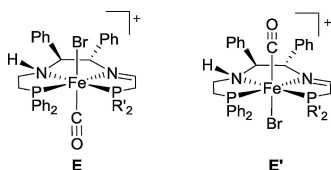


Figure 3. Geometries of the *trans* tetradentate complexes.

addition to a small fraction (17%) of two other isomers with poorly resolved doublet resonances at 62, 59 and 55 ppm (Table 1). These minor isomers might have the *cis-β* geometries shown in Figure 2 but this could not be definitively established. Similarly (**S,S**)-2 appears to have two *trans* isomers (75% of mixture) and at least one additional isomer at 58 and 63 ppm in the ³¹P{¹H} NMR spectrum. Each diastereomer has a characteristic set of doublets with ²J_{PP} ranging from 33 to 41 Hz (see Table 1). The use of the R' = iPr substituent led to a complex mixture of products. Attempts to make a complex with R' = 3,5-(CF₃)₂C₆H₄ by adapting a template synthesis method under acidic conditions^[6b] also led to a complex mixture. These will not be discussed here.

Table 1. ³¹P{¹H} NMR resonances of the *trans* isomers of **C1**, **C4**, (**S,S**)-1 and (**S,S**)-2 with structures **E** or **E'** of Figure 3.

Complex	PR' ₂	Isomer fraction (%)	PR' ₂ (ppm)	PPh ₂ (ppm)	² J _{PP} (Hz)	Struct.
C1	PPh ₂	100	62.6	58.0	40	E
C4	PCy ₂	75	78.4	47.3	33	E or E'
(S,S)-1-1	PEt ₂	38	65.1	59.3	38	E' or E
(S,S)-1-2	PEt ₂	45	67.1	53.7	36	E or E'
(S,S)-2-1	Po-Tol ₂	41	61.6	55.4	41	E or E'
(S,S)-2-2	Po-Tol ₂	34	63.7	54.1	39	E' or E

One relatively broad ($w_{1/2}$ 20 cm⁻¹) CO absorption (ν_{CO}) is observed in the IR spectrum for the iron(II) complexes as mixtures of isomers as listed in Table 2 for the two complexes as well as the complexes **C1** and **C4** for comparison (Table 2). Only one peak maximum representing an averaged electronic property of the various isomers present is reported because separate peak maxima were not resolved. There is no clear trend in the ν_{CO} values. The steric parameters of the PR'₂CH₂ group can be expressed in terms of Tolman's cone angles θ of the corresponding PR'₂Et ligands as also listed in Table 2.^[11]

Table 2. Stereoelectronic effects represented by Tolman's cone angle and IR wavenumbers of the CO ligand.

Complex	PR' ₂	IR ν_{CO} (cm ⁻¹)	Tolman's Cone Angle (θ) ^[a]
(S,S)-1	PEt ₂	1956	132
C1-Br ^[b]	PPh ₂	1979 ^[b]	141
C4	PCy ₂	1960	157
(S,S)-2	Po-Tol ₂	1963	173

[a] Cone angle of R'₂PEt representing the PR'₂CH₂ fragment of the complex. [b] Like **C1** from Figure 1, but synthesized with a bromo instead of a chloro ligand for better comparison.

2.2 Analysis of the Structures of the Isomers in Solution

Complex **C3** has been characterized crystallographically in the *trans* configuration with the NH locked *anti* with respect to the hydrogen of the adjacent CHPh group with (*S*) chirality as shown in Figure 1. All of the 43 racemic or enantiopure dppe metal derivatives in the Cambridge Crystallographic Databank have the NH and CH locked *anti* except for isomer **C4-S_{NH}** (see the Supporting information). The similarity of the NMR spectra of complexes **C1** to **C3** suggest that the major isomers all have this *trans* structure as do a wide variety of more symmetrical *trans*-[Fe(CO)Br(PR'₂-N-N-PR'₂)]⁺ complexes reported by our group with a wide range of substituents (Et, Cy, aryl).^[2,6]

The *cis-β* structure of **C4** in the solid state introduces another possibility for structural assignments and it has been observed in related iron and ruthenium complexes with tetradentate phosphorus and nitrogen ligands^[2b,12]. However in solution the main isomer of **C4** (75%) has the *trans* configuration with either the NH next to the CO ligand (structure **E**) or the Br ligand (**E'**) as in Figure 3. This is determined by assigning all of the protons around the backbone of the ligand using 2D NMR experiments and spin simulations and demonstrating the similarity to the proton spectra of *trans* complex **C1** (see the Supporting Information). In particular the ³J_{HH} coupling constants of the PPh₂CH₂CH₂NH part of the ligand backbone should be sensitive to the differences in dihedral angles between the *trans* and the *cis-β* configurations where this part of the tetradentate ligand that folds away from the PNN plane. The simulated ³J_{HH} couplings

are similar for the **C1**, (**S,S**)-**1** and **C4** isomers in the assigned *trans*-configuration. The large $^3J_{HH}$ coupling (12–14 Hz) indicative of *anti*-vicinal CH groups in the *trans* structure is present in the ^1H spectra of all of these compounds. The minor isomer of **C4** with $^{31}\text{P}\{^1\text{H}\}$ NMR signals at 76.0 and 75.5 ppm probably has a *cis*- β -**C4** structure, but it is in too low a concentration to provide definitive proton assignments. In another sample prepared for HMBC NMR analysis, another *trans*-isomer, (**E** or **E'**) with $^{31}\text{P}\{^1\text{H}\}$ NMR resonances at 73.0 (d) and 51.8 ppm (d, $^2J_{pp}$ 35 Hz) was also observed. Thus the $\text{PPh}_2\text{CH}_2\text{CH}_2$ arm of **C4** is mobile and allows a switch that is slow on the NMR timescale between the structures shown in Figure 2.

A ^1H - ^{31}P HMBC experiment and spin simulations were used to assign the structures of the *trans* isomers of complex (**S,S**)-**1**, although it was not possible to distinguish which of the two diastereomers was **E** vs **E'** of Figure 3 ($\text{PR}'_2 = \text{PEt}_2$). Table 1 lists the $^{31}\text{P}\{^1\text{H}\}$ chemical shifts and coupling constants of these isomers. Obtaining good NMR spectra for (**S,S**)-**2** was challenging but its $^{31}\text{P}\{^1\text{H}\}$ NMR spectra appear to be similar to those of (**S,S**)-**1**.

2.2 Catalytic Results

2.2.1 Acetophenone Reduction and Reaction Progress Modelling

The ATH of acetophenone (Figure 4) was carefully examined for catalysts (**S,S**)-**1**, (**S,S**)-**2** as well as **C1** and **C4** for comparison under a range of conditions.

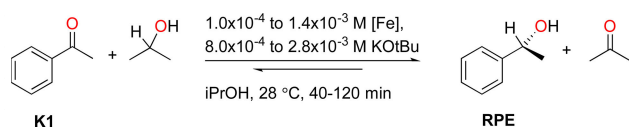


Figure 4. Conditions for the ATH of acetophenone.

Initial catalytic reactions were done with acetophenone (**K1**) with a precatalyst/KOtBu/substrate ratio (C/B/S) of 1/2/500 with [**K1**] 0.70 M in iPrOH at 28 °C. Figure 5 shows that complexes (**S,S**)-**1** with the small PEt_2 group reduces acetophenone to 1-phenylethanol to the equilibrium point of 86% conversion with a high initial TOF of approx. 12 s^{-1} as determined by reaction profile fitting (see below). The conversion can be increased to over 90% by using a lower concentration of ketone (e.g. 0.1 M). The complexes **C4** and (**S,S**)-**2** with bulkier PCy_2 and Po-Tol_2 groups have lower initial TOF and lose activity before reaching equilibrium. On the other hand the last two complexes maintain a high ee in the product while (**S,S**)-**1** has significant losses in ee over time because of its poor selectivity. There is less ee degradation over the course of the reaction when using a lower catalyst loading^[3b] with the C/B/S ratio 1/8/6121 with [ketone] 0.63 M

(Figure 6). **C4** and (**S,S**)-**2** were again slower than (**S,S**)-**1** at reducing acetophenone; however the ee for **C4** was much higher (98% *R*) at maximum conversion. The reaction slows after 40% conversion and attains only 80% of the possible conversion at 120 min. This is also true for (**S,S**)-**2**. This is attributed to some modification of the active catalyst over time. (**S,S**)-**2** produces the alcohol in 89% ee (*R*) after 120 minutes. (**S,S**)-**1** has the higher activity to a maximum conversion of 87% after 50 min, but also a lower ee of 85%. For comparison **C1** with PPh_2 groups produces 1-phenylethanol at 82% ee at the time of maximum conversion.^[3b]

The reaction progress and changes in ee for the ATH of acetophenone (AP) were semi-quantitatively fit for the first time to a simple kinetic model^[13] for a reversible equilibrium using the program Dynafit^[14] (Figures 7–10). The progress of the reactions catalyzed by (**S,S**)-**1**, (**S,S**)-**2**, **C1** and **C4** were fit to only three parameters: two rate constants k_R and k_S for pseudo first order reactions producing (*R*)- and (*S*)-1-phenylethanol (abbreviated RPE and SPE, respectively) and one equilibrium constant ($K_{\text{rac}} = 2k_R/k_{-R} = 2k_S/k_{-S}$) for the reversible reaction of acetophenone with isopropanol to give 1-phenylethanol and acetone. The same $K_{\text{rac}} = 12$ applies to all of the reactions of Figures 5 and 6. From the rate constants the intrinsic enantioselectivity of the catalyst is obtained ($S = k_R/k_S$).^[13] The value of S determines the initial ee of the system. The initial TOF is given by $(k_R + k_S)[\text{AP}]/[\text{Cat}]$ and the initial e.e. (%) is given by $100(k_R - k_S)/(k_R + k_S) = 100(S - 1)/(S + 1)$.

This simple approach makes the following assumptions:

1. The forward reaction to produce RPE is first order in AP with a steady-state catalyst concentration included in the rate constant k_R .
2. The forward reaction to produce SPE is first order in AP with a steady-state catalyst concentration included in the rate constant k_S .
3. At equilibrium, the concentrations of RPE and SPE will be equal (0 ee) and the equilibrium constant will be $K_{\text{rac}} = 2K_R = 2K_S = 12.0$ for the conditions described here.
4. The backward reaction to produce AP from RPE is first order in RPE with a steady-state catalyst concentration included in the rate constant $k_{-R} = k_R/K_{\text{rac}} = 2k_R/K_{\text{rac}}$.
5. The backward reaction to produce AP from SPE is first order in SPE with a steady-state catalyst concentration included in the rate constant $k_{-S} = k_S/K_{\text{rac}} = 2k_S/K_{\text{rac}}$.

Assumptions 4 and 5 explain why the ee of the product degrades with the progress of the reaction if k_S is non-negligible.

The model was validated using data from the well-defined catalyst **C1** (Figure 7). The parameters obtained are listed in Table 3. Catalyst **C1** with two moderately sized PPh_2 groups has an extremely high TOF of 250 s^{-1} as documented elsewhere^[3b] and an inherent selectivity S of 12, resulting in a starting ee of 85% which degrades to 78% at maximum conversion at 120 s. The experimental ee have larger uncertainties early in the reaction because of the low concentration of the (*S*)-1-phenylethanol in the sample but the model fits the general trends in the ee.

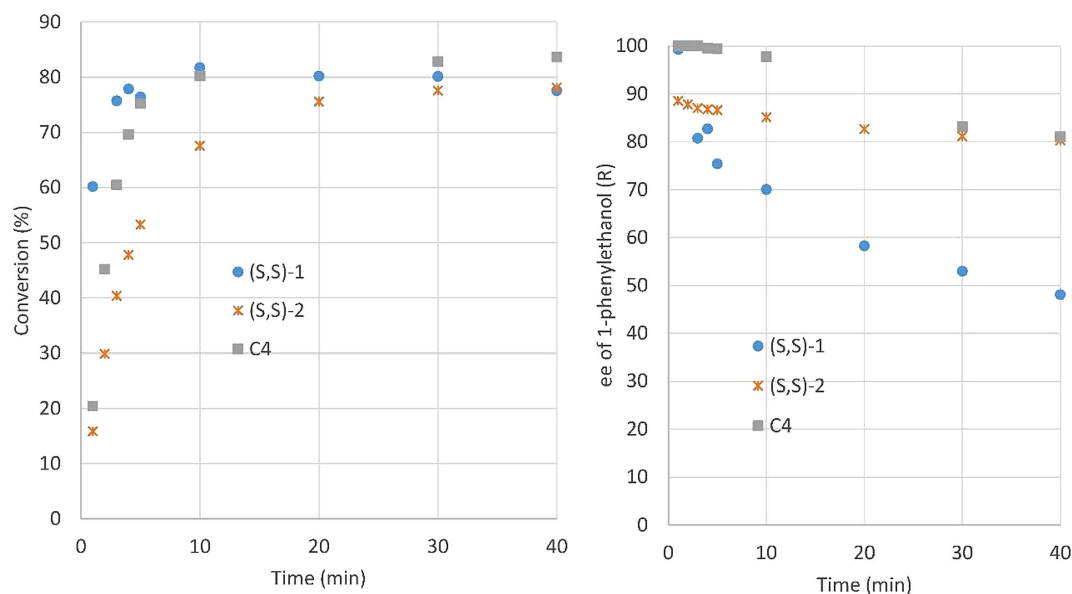


Figure 5. ATH of acetophenone (**K1**) with **(S,S)-1**, **(S,S)-2** and **C4**. Reaction conditions: 28 °C, 1.4×10^{-3} M precatalyst, 2.8×10^{-3} M KOtBu, 0.70 M acetophenone, 6 mL iPrOH, C/B/S=1/2/500; % conversion and % ee determined by chiral GC.

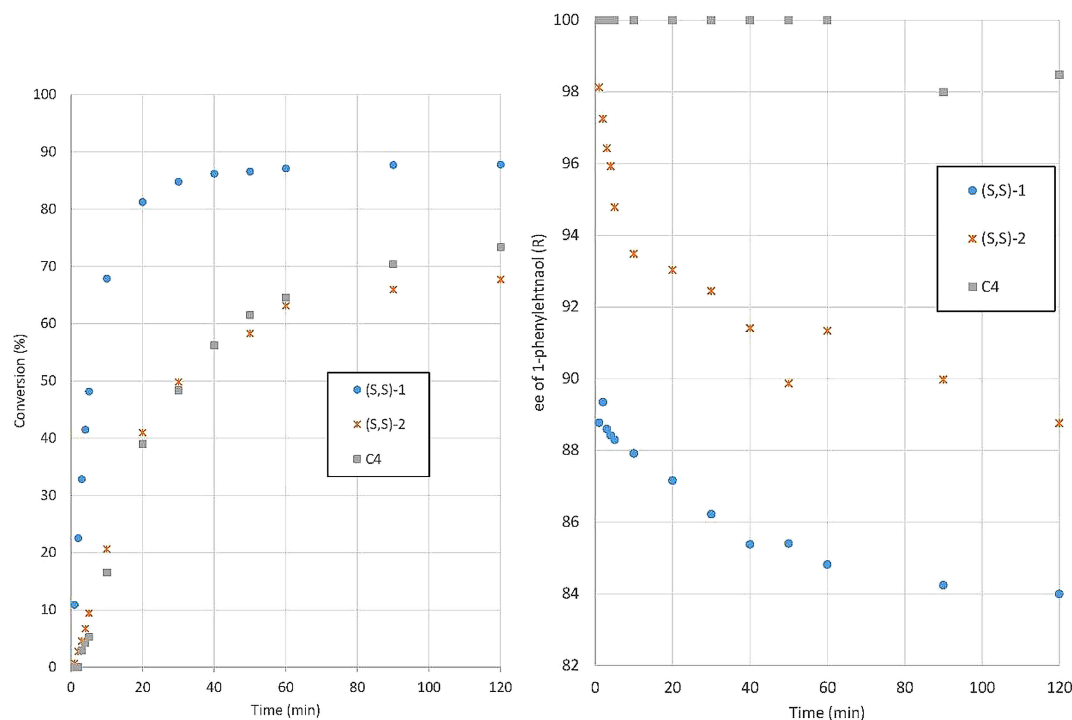


Figure 6. ATH of **K1** with **(S,S)-1**, **(S,S)-2** and **C4**. Reaction conditions: 28 °C, 1.0×10^{-4} M precatalyst, 8×10^{-4} M KOtBu, 0.63 M acetophenone, 6 mL iPrOH, C/B/S=1/8/6121; % conversion and % ee determined by chiral GC.

The fits to the reaction progress for **(S,S)-1** (Figure 8) show that this system is slower (TOF 14 s^{-1}) than **C1** but more enantioselective ($S = 20$). Thus there are dramatic effects in changing one PPh_2 (on **C1**) with one PET_2 group.

(S,S)-2 and **C4** do not fit the simple model (Figures 9 and 10). The reactions slow more than expected with conversion and this indicates that the catalyst concentration is being reduced over the course of the catalytic run. This may be due to inhibition due to binding of the product alcohol. It is interesting that for **(S,S)-2**, the ee drops rapidly from a high

value of 99% *R* over the course of the first 250 seconds. This is modelled by a more enantioselective catalyst ($S = 200$) being completely replaced by a less selective one (with $S = 28$) over this time period. This is likely to be caused by the dissociation and repositioning of the bulky $\text{CHCHP}(\text{o-Tol})_2$ arm of the ligand in an as-of-yet, undefined way. Complex **C4** with the slightly smaller PCy_2 group is more stable and produces the alcohol in exceptionally high ee up to maximum conversion.

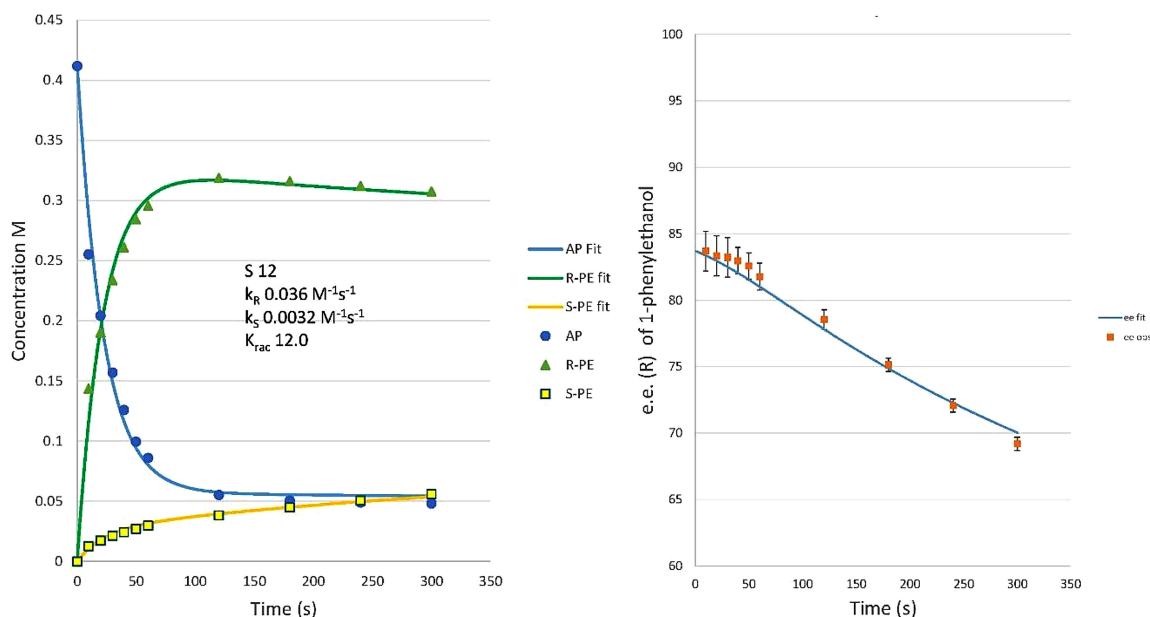


Figure 7. (Left) Kinetic fit to the changes in concentration in the ATH of acetophenone catalyzed by **C1**. (Right) Fit to the changes in ee for the reaction.

Table 3. Results of fitting the reaction profiles.¹

Catalyst	k_R (s ⁻¹)	k_S (s ⁻¹)	TOF (s ⁻¹)	<i>S</i>	ee initial (% R)	ee (at time in min)	TON
C1 ²	3.6e-2	3.2e-3	235	12	85	78 (2)	5900
(S,S)-1	2.1e-3	1.1e-4	14	20	90	80 (40)	5000
(S,S)-2 ³	4.0e-4	2.0e-6	6	200	99	93 (4)	500
(S,S)-2 ³	4.1e-4	1.7e-5	3	28	92	90 (90)	3700
C4	4.5e-4	1e-6	3	510	99.6	98.5 (120)	4400

¹ [FeBr(CO)(PR'₂CH₂CHNCHPhCPhNHCH₂CH₂PPh₂)]BPh₄: [Cat]=1.05e-4 M, [KOtBu]=8e-4 M, [AP]=0.63 M, 28 °C in isopropanol, K_{rac} =12.0. ² [FeCl(CO)(PPh₂CH₂CHNCHPhCPhNHCH₂CH₂PPh₂)]BF₄: [Cat]=6.8e-5 M, [KOtBu]=5.4e-4 M, [AP]=0.41 M, 28 °C in isopropanol, K_{rac} =12.0. ³ There is a change in catalyst structure over the course of the first 250 seconds.

The TOF and *S* values obtained from fitting the reaction profiles are plotted as a function of the cone angle of the PR'₂-CH₂ group in the complex (Figures 11 and 12). Variations in the electronic environment as reflected in the ν (CO) of the complexes are too small to show a meaningful variation with TOF or *S*. As far as activity (TOF) is concerned there is a region in the plot around the size of the PPh₂ group where the TOF is high (Figure 11). The PPh₂ complex **C1** is an order of magnitude more active than the PEt₂ and PiPr₂ complexes. The use of bulky PCy₂ and Po-Tol₂ groups result in lower TOF. This is consistent with our earlier stereoelectronic study of precatalysts **B** (Figure 1) indicating that both studies reflect the actual activity of the catalyst and not the activation of the precatalyst; an induction period was observed for catalysis with **B** because an imine in **B** has to be reduced to an amine^[3a]

while no induction period is observed for the catalyst systems discussed here.

However as far as the intrinsic enantioselectivity *S* is concerned, it rises from less than 20 for the smaller substituents (PEt₂, PPh₂) to a maximum of 510 for bulky PCy₂ (98 % ee) and then falls again to 200 and then to 28 for the very bulky Po-Tol₂ as discussed above (Figure 12).

2.2.2 Other Substrates

The ATH of a range of ketones shown in Figure 13 were tested for the complexes, **(S,S)-1** and **(S,S)-2** (Figure 14). All of the catalytic results from this study were compared to those of **C4**, and those of **C1**, retested under the conditions of the present study for ease of comparison.

The best results are summarized in Table 4; a more complete Table can be found in the SI. Included are results for **C4** as reported elsewhere.^[3c] All of the chiral alcohol products are enriched in the *R*-enantiomer which is consistent with our previous findings.^[3b,c,15]

First the series of substrates with one phenyl group and one R group of increasing size (H to Me to Et to iPr) are considered. All of the complexes quantitatively convert benzaldehyde (**A1**) to benzyl alcohol within a few minutes. The reduction of propiophenone, **K2**, is achieved with around 80% conversion for each complex. Complexes **C4** and **(S,S)-2** with the bulky substituents make product with ee greater than 90% ee while **(S,S)-1** is less enantioselective (86% ee) but much more active; **C1** produces a low ee product. The bulkier **K3**, *i*-butyrophenone, is only reduced by **(S,S)-1** and **C1** with the smaller PR'₂ substituents ($\theta < 142^\circ$) but the enantioselectivity

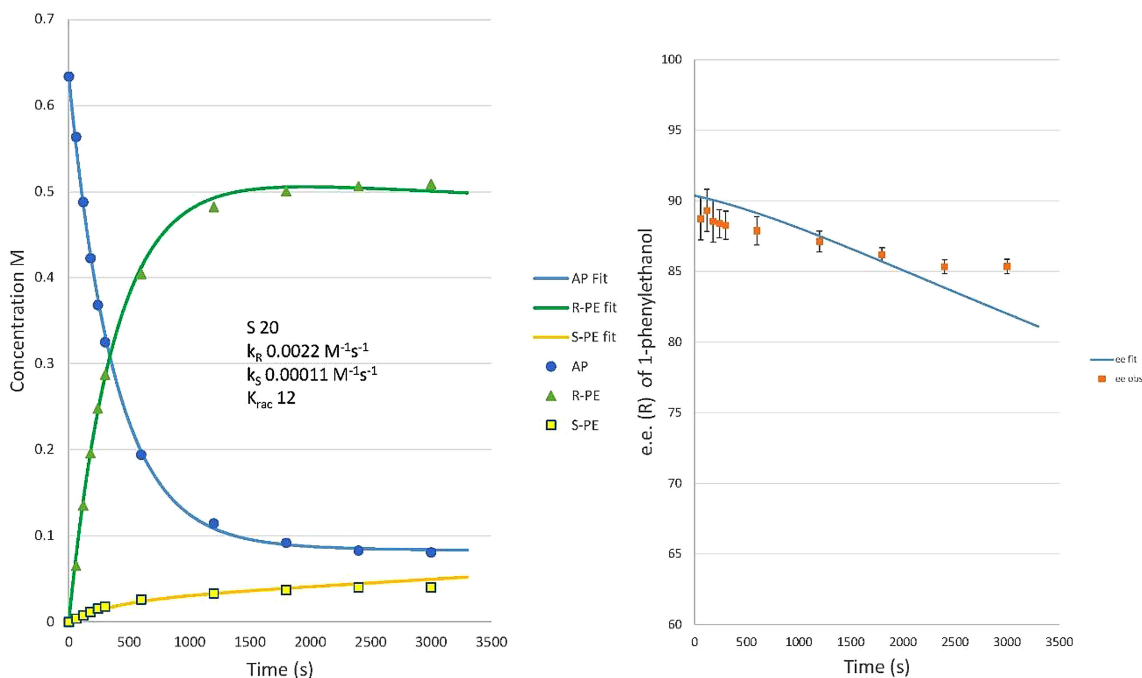


Figure 8. Simulation of the reaction progress of (S,S)-1 of Figure 6.

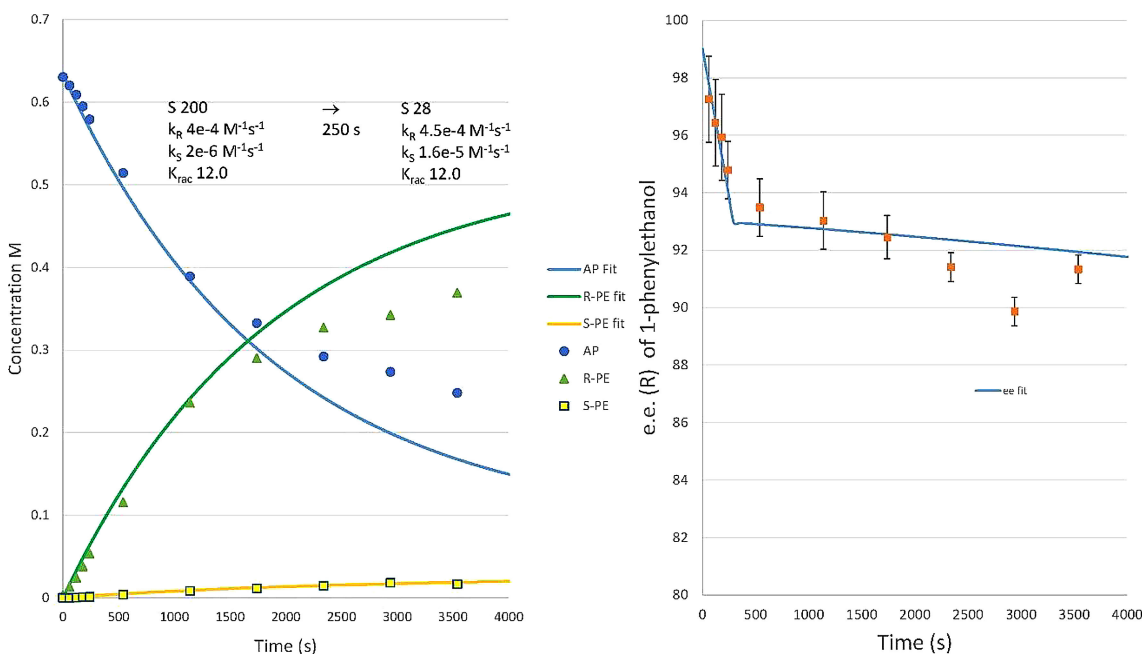


Figure 9. Simulation of the reaction progress of (S,S)-2 of Figure 6. The catalyst is converted over 250 s from one that is very enantioselective ($S=200$) to one that is less ($S=28$).

tivity is poor; this suggests that the active sites of the other catalysts are too restricted in size.

The series of methylketones MeCOAr (**K4** to **K9**) provide a range of functional groups to test the catalysts. The reduction of **K4** and **K5** with chloro substituents on the phenyl ring is

achieved with high conversions, with the *ortho*-chloro substituent in **K5** producing much higher ee (84-94% depending on the catalyst) than with the *para*-chloro group in **K4** (6-58% ee). High enantiopurity is beneficial for the production of (*R*)-2'-chloro-1-phenylethanol as it is a key intermediate for a

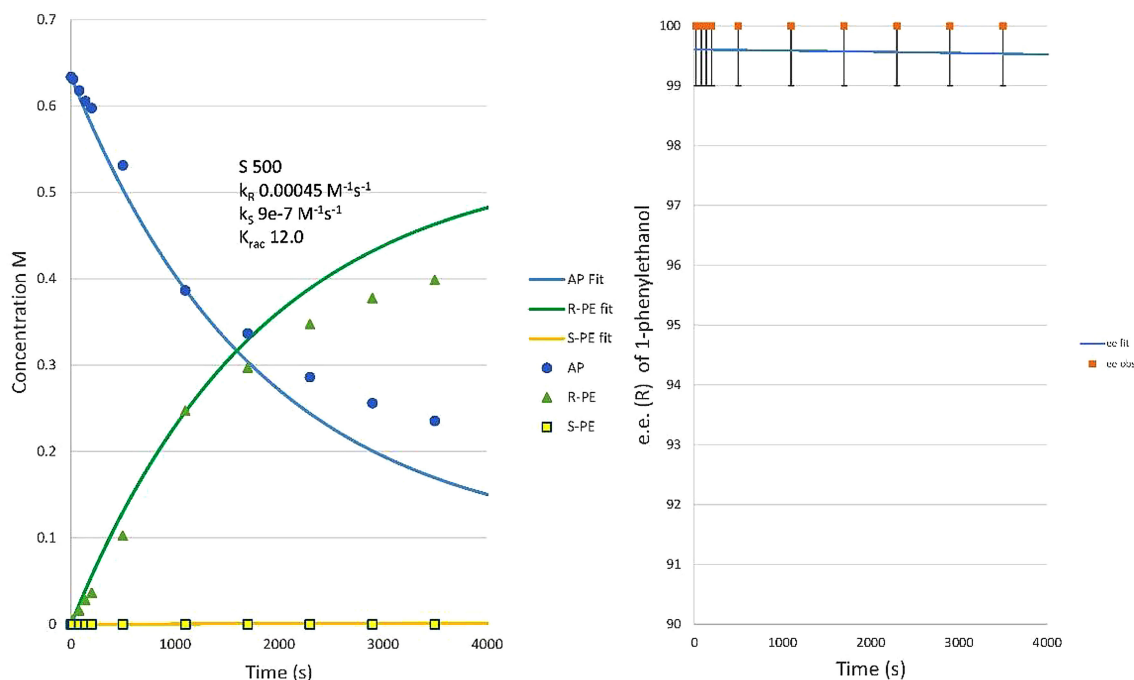


Figure 10. Simulation of the reaction progress of **C4** of Figure 6.

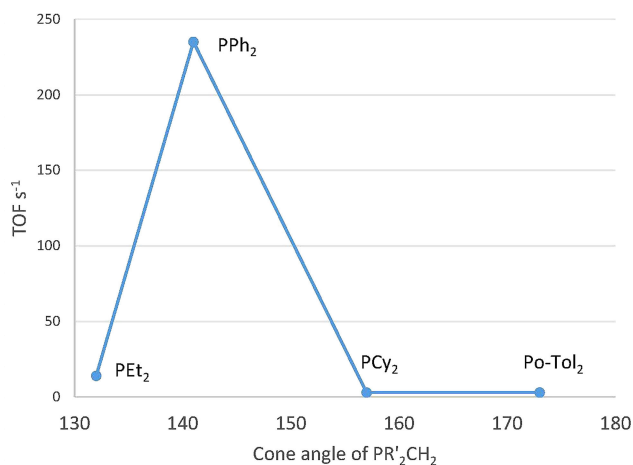


Figure 11. TOF (s^{-1}) for the ATH of acetophenone catalyzed by complexes as a function of cone angle ($^{\circ}$) of the PR'_2 group (see Tables 2 and 3). Reaction conditions are as in Figure 6

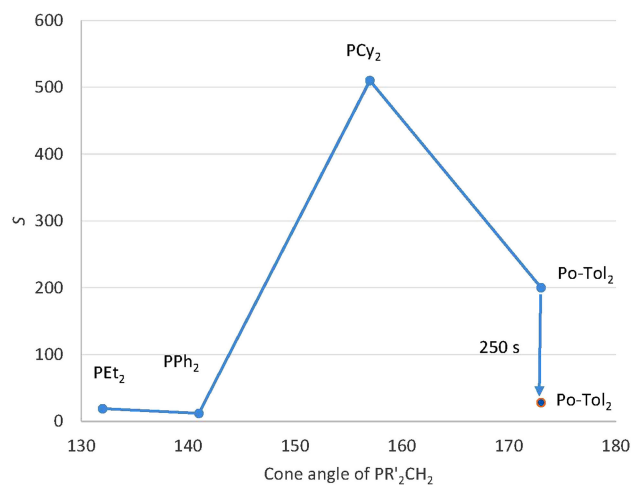


Figure 12. The intrinsic enantioselectivity $S = k_R/k_S$ for the ATH of acetophenone catalyzed by **(S,S)-1**, **(S,S)-2**, **C1** and **C4** as a function of cone angle ($^{\circ}$) of the PR'_2CH_2 group. Reaction conditions are as in Figure 6. The selectivity of **(S,S)-2** drops over the first 250 s of the reaction.

chemotherapeutic drug.^[16] The *bis*- CF_3 -substituted arylketone **K6** is fully reduced to the alcohol in $>90\%$ ee by **C1** and **(S,S)-2** that contain PAR_2 groups while **(S,S)-1** with a more basic PEt_2 group appears to be deactivated by the acidic alcohol product after 40–60% conversion. The enantiopure alcohol is valuable as it is a key intermediate for the synthesis of Aprepitant.^[17] *Para*-methylacetophenone (**K7**) was more difficult to reduce than the chloro analogue, and relatively low ee are achieved. The presence of a potentially coordinating

pyridyl group in **K8** is conducive, not detrimental, to the complete reduction of the ketone. However, the furan in **K9** deactivates all of the complexes except **C1**.^[3b] 3-Methyl-2-butanone (**K10**) is reduced to 90% conversion but with low ee by **C1**, while both **C4** and **(S,S)-2** are less active but give higher ee at 43% and 55%, respectively. The complete reduction of cyclohexanone (**K11**) is achieved with **(S,S)-2** and **C1**, while only partial conversion is observed for **(S,S)-1**.

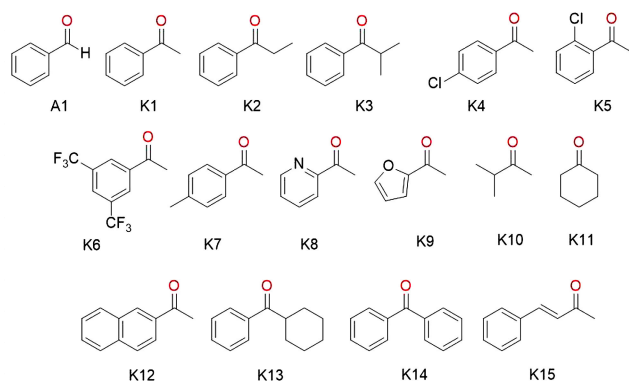


Figure 13. Substrate scope for ATH using complexes **(S,S)-1**, **(S,S)-2**, **C1** and **C4**.

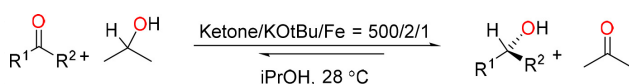


Figure 14. Conditions of ATH catalysis.

C4 is the most enantioselective catalyst for the ATH of the 2-naphthyl ketone **K12** with 82% ee, and it was the only complex that successfully reduced cyclohexylphenyl ketone (**K13**), although with only 11% conversion. All of the catalysts reduce benzophenone (**K14**) efficiently. The presence of a C=C bond in benzylidene acetone (**K15**) proved to be a complicating factor as all of the complexes with the exception of **(S,S)-2** are unselective and reduced both the C=O and C=C bonds. For the unselective catalysts, the GC traces show the three possible reduction products of C=O reduction, C=C reduction, and both, even at 1 min, with the fully reduced product growing in over time. **(S,S)-2** is selective for the formation of the allyl alcohol product with less than <1% conversion to the doubly saturated product after 60 min. In summary, while **C1** is a very active catalyst with a high TOF, replacing one of its PPh₂ groups with a PCy₂ group results in a more enantioenriched alcohol for all of the ketones except **K5**. The change to a P(o-Tol)₂ group gave superior ee for **K2**, **K4**, **K6** and **K10**. Surprisingly even the small PEt₂ group of **(S,S)-1** provided comparable or greater enantioselectivity to that of the PPh₂ group in complex **C1** for **K2**, **K4**, **K7** and **K10**.

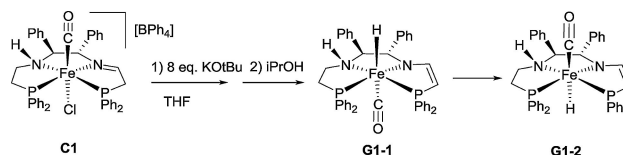
2.3 Observation of Hydride Species

The precatalyst solution of **C4** was treated with base and iPrOH in order to characterize possible catalytically active species by use of NMR and IR spectroscopy as has been done already for **C1**.^[3b] When **C1** was treated by first the addition of KOtBu in THF, then evaporation, dissolution in C₆D₆, a mixture of amido-enamido complexes was identified.^[3b] Then the addition of iPrOH produced first, a transient hydride isomer **G1-1** (Scheme 2) which rearranged over time to a

Table 4. Results for the ATH of ketones in Figure 13 using complexes **C1**, **(S,S)-1** to **(S,S)-2**, and previously reported results using **C4**.^[a]

Entry	Substrate ^[b]	Precatalyst	Conv. (%) ^[c]	Time (min)	ee (%) ^[c]	TON
1	K2	(S,S)-2	82	30	90	410
2		C4	80	60	94	400
3		(S,S)-1	79	3	86	395
4	K3	(S,S)-1	52	60	12	260
5		C1	88	40	40	440
6	K4	C4	92	10	52	460
7		(S,S)-2	92	10	58	460
8	K5	(S,S)-1	> 99	1	90	500
9		C4	> 99	10	94	500
10		C1	> 99	1	94	500
11	K6	(S,S)-2	> 99	30	93	500
12		C1	> 99	1	91	500
13	K7	(S,S)-2	60	40	63	300
14		C4	60	20	65	300
15	K8	(S,S)-1	> 99	3	N/A	500
16		(S,S)-2	> 99	5	N/A	500
17		C1	> 99	2	N/A	500
18	K9	(S,S)-1	0	60	N/A	0
19	K10	C4	44	60	43	220
20		(S,S)-2	75	40	55	375
21		C1	90	20	23	450
22	K11	(S,S)-1	33	60	N/A	165
23		(S,S)-2	> 99	2	N/A	500
24		C1	> 99	50	N/A	500
25	K12	(S,S)-1	81	30	23	405
26		C4	88	40	82	440
27		(S,S)-2	84	40	59	420
28	K13	C4	11	60	53	55
29	K14	(S,S)-1	90	20	N/A	450
30		C4	89	20	N/A	445
31		(S,S)-2	91	20	N/A	455
32		C1	89	1	N/A	445
33	K15	(S,S)-2	22	30	46	110

[a] Reaction conditions: 28 °C, 8.9x10⁻² mmol catalyst, 0.18 mmol KOtBu, 44.3 mmol substrate, 6 mL iPrOH. [b] C/B/S = 1/2/500. [c] % conversion and % ee determined by chiral GC.

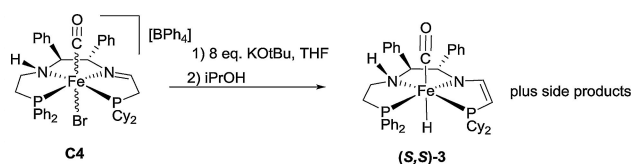


Scheme 2. Generation of Iron(II) Hydride Species Starting with **C1** as Reported Previously

second isomer **G1-2**. Based on NOE studies, isomer **G1-1** has a *trans* configuration with the Fe–H group parallel to the N–H group while **G1-2** is thought to have the *trans* configuration with Fe–CO moiety parallel to the N–H group.^[3b]

The precatalyst **C4** was mixed with 8 equivalents of KOtBu in THF for 5 min, then dried *in vacuo* and dissolved in C₆D₆. The solution at this stage produce complicated NMR spectra with features reported previously for amido-eneamido

complexes generated from **C1** (see the Supporting Material).^[3b,7,15] The mixture of complexes was then dissolved and stirred in ⁱPrOH for 1 min, or until the residue was completely dissolved. It was then dried immediately affording the new hydride species *trans*-(*S,S*)-**3** (Scheme 3, Table 5). Its NMR properties are similar to those of hydride **G1-2** and so we tentatively assign the structure as *trans* with the NH parallel to the FeCO group. The ³¹P{¹H} NMR resonances associated with these hydride complexes have ²J_{PP} 25–27 Hz, consistent with *cis* phosphorus nuclei (Table 5). **G1-2** and *trans*-(*S,S*)-**3** show a similar doublet of doublet hydride pattern in the region of –9.3 to –10.3 ppm with ²J_{PH} of 59–60 and 80–82 Hz. These coupling constants are typical of *cis* phosphorus and hydride nuclei on Fe(II) and thus the stereochemistry of these hydride complexes is likely to be *trans*. In all cases found so far, the magnitude of ²J_{P-Fe-H}^{trans} is smaller than that of ²J_{P-Fe-H}^{cis} for terminal iron hydride complexes: ²J_{P-Fe-H}^{trans} is in the range 12–35 Hz^[18] whereas ²J_{P-Fe-H}^{cis} is in the range 30–85 Hz.^[18a-e,1,19] In some instances the ²J_{P-Fe-H}^{trans} and ²J_{P-Fe-H}^{cis} in iron hydride polyphosphine complexes are averaged to a small value due to nuclear exchange caused by molecular fluxionality.^[20]



Scheme 3. Generation of Iron(II) Hydride Species (*S,S*)-**3**

Table 5. NMR properties of the hydride complexes

Precursor to Hydride Complex	PR' ₂	δ ³¹ P (ppm)	² J _{PP} (Hz)	δ ¹ H (ppm)	² J _{HP} (Hz)
C1 hydride	PPh ₂	84.9,	33.2	-2.3	71, 62 ^a
G1-1		70.4			
C1 hydride	PPh ₂	75.7,	27.5	-9.2	80, 60 ^b
G1-2		71.4			
(S,S)-3	PCy ₂	91.2,	36.6	-10.3	82.2,
		83.0			59.8

^a previously reported as 70 Hz^[3b] ^b previously reported as 79 Hz^[3b]

Treating (*S,S*)-**1** and (*S,S*)-**2** in a similar fashion also produces hydride resonances in this region but the hydrides are very reactive and unstable so that the ³¹P{¹H} NMR spectra are complex with some unidentified species and signals for uncoordinated phosphorus species.

Thus hydride complex *trans*-(*S,S*)-**3**, like **G1-2**, is thought to have the NH of the ligand parallel to the Fe-CO group and not in a suitable position for an outersphere hydride and proton attack on the ketone.^[3b]

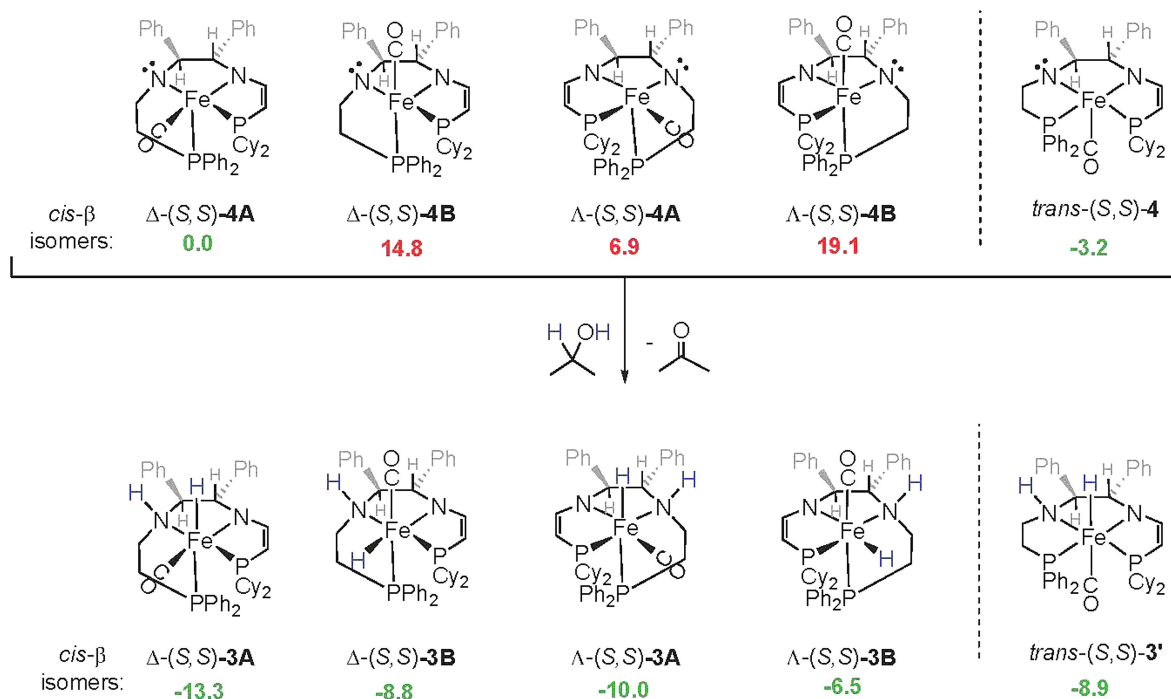
3 Density Functional Theory Calculations

Due to the difficulties in establishing the coordination geometries of the products upon reacting **C4** with base, we employed Density Functional Theory to compare relative ground state energies of various diastereomers. Details of the calculations and the three dimensional Cartesian coordinates are provided in the Supporting Information. The calculated geometries of *cis*-β complexes **C4-R_{NH}** and **C4-S_{NH}** correspond well with the X-ray structural data reported previously for **C4**,^[8] with **C4-S_{NH}** being only 1.8 kcal/mol higher in energy (SI, Scheme S1). The *cis*-β stereochemistry of the two diastereomers can be further characterized as Δ-*cis*-β-**C4-R_{NH}** and Λ-*cis*-β-**C4-S_{NH}**. Deprotonation of **C4** with at least two equivalents of base could lead to the formation of at least four possible amido-eneamido complexes (*S,S*)-**4** (Scheme 4) and the *trans*-amido structure by analogy to mechanistic studies based on **C1**.^[15,21] We found that the *trans*-(*S,S*)-**4** isomer is slightly lower in energy (3.2 kcal/mol) relative to the Δ-*cis*-β-(*S,S*)-**4** amido complex (Scheme 4). The *trans* isomer can produce, via the transfer of a proton/hydride equivalent from ⁱPrOH, the high energy, catalytically active, octahedral, FeH-NH complex, *trans*-(*S,S*)-**3'**, with FeH and NH parallel as proposed for the *trans*-amido-eneamido from **C1**. In the absence of substrate, the formation of the hydride Δ-*cis*-β-(*S,S*)-**3A** is calculated to be most favorable (-13.3 kcal/mol) among the various *cis*-β structures. The relative energy of the kinetically-formed hydride complex *trans*-(*S,S*)-**3'** is calculated to be -8.9 kcal/mol, 4.4 kcal/mol higher than the Δ-*cis*-β isomer and 2 kcal/mol higher than the observed hydride (*S,S*)-**3**.

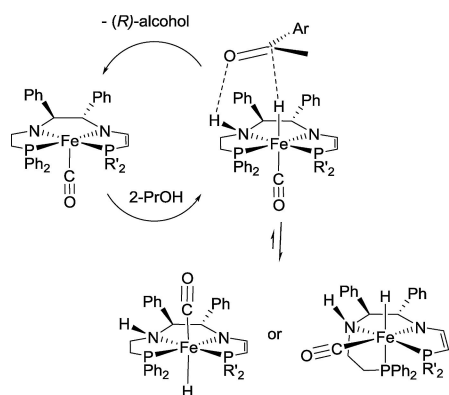
4. Proposed Mechanism

Thus, we suggest that the activity of the system is determined by the relative stability of a catalytic *trans*-hydride like *trans*-(*S,S*)-**3'** and the off cycle *trans* hydride *trans*-(*S,S*)-**3** or Δ-*cis*-β-(*S,S*)-**3** hydride species and of the catalytic *trans* amido-eneamido species as indicated in Scheme 5. The larger and/or more basic PR'₂ groups favor the off-cycle structures and thus are less reactive. The similarity of the structure of the ketone adduct with the unobserved active hydride (Scheme 5) to that of the one proposed for the PPh₂ catalyst system **C1**^[15,21] could explain why the (*R*)-aryl alcohols are produced by the *trans*-(*S,S*)-hydride catalysts using a transition state structure similar to that described for **C1**.^[15,21]

DFT calculations (see SI) indicate that **G1-2** may have a Δ-*cis*-β geometry for the off-cycle structure shown in Scheme 5; this structure is 3 kcal/mol more stable than the *trans*-isomer **G1-1**. Thus it is possible that the off-cycle hydride complexes with a Δ-*cis*-β geometry rearrange to low concentration catalytically active isomers with the NH and FeH parallel as shown in Scheme 5.



Scheme 4. Ground state energy comparison of some isomers of Cy-amido complexes (**(S,S)-4**) and the hydride isomers (**(S,S)-3**) derived from them by reaction with 2-PrOH. All energies are given in kcal/mol and relative to Δ -*cis*- β -(**(S,S)-4**) plus relevant small molecules. M06 L/TZVP/TZVPfit-IEF-PCM(THF).



Scheme 5. Proposed mechanism for the ATH catalyzed by complexes (**(S,S)-1**), (**(S,S)-2**), **C1** and **C4**. The observed hydride *trans*-(**(S,S)-3**) when R' is Cy is proposed to be off cycle.

5. Summary

In conclusion, two new precatalyst complexes have been synthesized with different steric and electronic properties at one phosphine (PEt_2 vs Po-Tol_2) coordination site of our third generation iron(II) (P-NH-N-P') system. These have been tested in the catalytic ATH of ketones and compared to the previously reported complexes **C1** and **C4**. The progress of the catalytic reactions could be fit for the first time to a simple three parameter kinetic model which describes the activity and

degradation of ee over the course of the reaction. We found that by increasing the steric bulk at one phosphine, the enantioselectivity increases (to greater than 98% in case of **C4**) with a concomitant decrease in activity.

This work provides evidence for a correct matching of catalyst structure with substrate structure to produce superior activity and selectivity. The bulky isobutyrophenone (**K3**) is only reduced by (**(S,S)-1**) and **C1** probably because these catalysts have the small PEt_2 or PPh_2 groups. Surprisingly (**(S,S)-1**) provides (*R*)-1-*ortho*-chlorophenylethanol in high ee (90%) from **K5**, despite the small size of the PEt_2 group. Cyclohexanone (**K11**) was only reduced by the (**(S,S)-2**) and **C1** catalyst systems. We also found that the steric and electronic properties can be varied to introduce chemoselectivity, as in the case of the selective C=O reduction of benzylidene acetone by complex (**(S,S)-2**) and none other.

We provided spectroscopic and computational characterization of hydride complexes that provide an understanding of the mechanism of the catalytic ATH using these iron complexes.

Acknowledgements

NSERC Canada is thanked for a Discovery Grant to RHM and scholarship funding to DEP. SAM thanks Digital Specialty Chemicals Ltd. for an OGSST Scholarship. The authors acknowledge the Canadian Foundation of Innovation, project

number 19119, and the Ontario Research Fund for funding of the Centre for Spectroscopic Investigation of Complex Organic Molecules and Polymers and Compute Canada for providing computational resources.

References

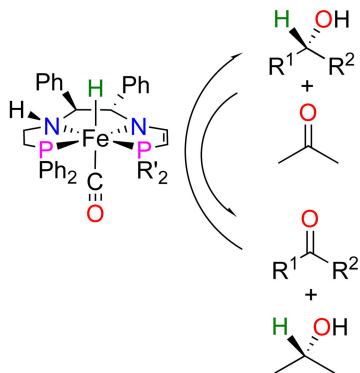
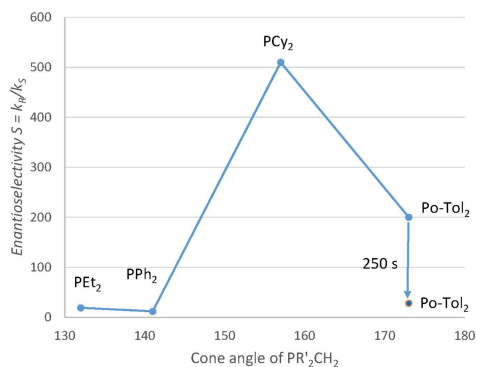
- [1] a) L. Cotarca, M. Verzini, R. Volpicelli, *Chimica Oggi-Chem. Today* **2014**, *32*, 36–41; b) P. Dupau, in *Organometallics as Catalysts in the Fine Chemical Industry, Vol. 42* (Eds.: M. Beller, H. U. Blaser), Springer-Verlag, Berlin, **2012**, pp. 47–63; c) R. Noyori, *Adv. Synth. Catal.* **2003**, *345*, 15–32; d) L. A. Saudan, *Acc. Chem. Res.* **2007**, *40*, 1309–1319.
- [2] a) J. S. Chen, L. L. Chen, Y. Xing, G. Chen, W. Y. Shen, Z. R. Dong, Y. Y. Li, J. X. Gao, *Acta Chimica Sinica (Huaxue Xuebao)* **2004**, *62*, 1745–1750; b) R. Bigler, R. Huber, A. Mezzetti, *Synlett* **2016**, *27*, 831–847; c) R. Bigler, A. Mezzetti, *Org. Process Res. Dev.* **2016**, *20*, 253–261; d) T. Bleith, H. Wadepohl, L. H. Gade, *J. Am. Chem. Soc.* **2015**, *137*, 2456–2459; e) F. Foubelo, C. Nájera, M. Yus, *Tetrahedron Asymmetry* **2015**, *26*, 769–790; f) J. P. Hopewell, J. E. D. Martins, T. C. Johnson, J. Godfrey, M. Wills, *Org. Biomol. Chem.* **2012**, *10*, 134–145; g) Y. Y. Li, S. L. Yu, W. Y. Shen, J. X. Gao, *Acc. Chem. Res.* **2015**, *48*, 2587–2598; h) R. H. Morris, *Chem. Soc. Rev.* **2009**, *38*, 2282–2291; i) R. H. Morris, *Acc. Chem. Res.* **2015**, *48*, 1494–1502; j) A. Naik, T. Maji, O. Reiser, *Chem. Commun.* **2010**, *46*, 9265–9265; k) B. Stefane, F. Pozgan, *Catal. Rev. Sci. Eng.* **2014**, *56*, 82–174; l) P. E. Sues, K. Z. Demmans, R. H. Morris, *Dalton Trans.* **2014**, *43*, 7650–7667; m) S. L. Yu, W. Y. Shen, Y. Y. Li, Z. R. Dong, Y. Q. Xu, Q. Li, J. N. Zhang, J. X. Gao, *Adv. Synth. Catal.* **2012**, *354*, 818–822.
- [3] a) A. A. Mikhailine, M. I. Maishan, A. J. Lough, R. H. Morris, *J. Am. Chem. Soc.* **2012**, *134*, 12266–12280; b) W. Zuo, A. J. Lough, Y. Li, R. H. Morris, *Science* **2013**, *342*, 1080–1083; c) S. A. M. Smith, R. H. Morris, *Synthesis* **2015**, *47*, 1775–1779; d) R. Bigler, R. Huber, A. Mezzetti, *Angew. Chem. Int. Ed.* **2015**, *54*, 5171–5174; e) R. Bigler, A. Mezzetti, *Org. Lett.* **2014**, *16*, 6460–6463; f) R. Bigler, E. Otth, A. Mezzetti, *Organometallics* **2014**, *33*, 4086–4099.
- [4] C. Sui-Seng, F. Freutel, A. J. Lough, R. H. Morris, *Angew. Chem. Int. Ed.* **2008**, *47*, 940–943.
- [5] J. F. Sonnenberg, N. Coombs, P. A. Dube, R. H. Morris, *J. Am. Chem. Soc.* **2012**, *134*, 5893–5899.
- [6] a) P. O. Lagaditis, A. J. Lough, R. H. Morris, *Inorg. Chem.* **2010**, *49*, 10057–10066; b) P. E. Sues, A. J. Lough, R. H. Morris, *Organometallics* **2011**, *30*, 4418–4431.
- [7] W. Zuo, S. Tauer, D. E. Prokopchuk, R. H. Morris, *Organometallics* **2014**, *33*, 5791–5801.
- [8] S. A. M. Smith, A. J. Lough, R. H. Morris, *UICrData* **2017**, <https://doi.org/10.1107/S2414314617004527>.
- [9] W. Zuo, R. H. Morris, *Nature Prot.* **2015**, *10*, 241–257.
- [10] A. A. Mikhailine, P. O. Lagaditis, P. Sues, A. J. Lough, R. H. Morris, *J. Organometal. Chem.* **2010**, *695*, 1824–1830.
- [11] C. A. Tolman, *Chem. Rev.* **1977**, *77*, 313–348.
- [12] R. Bigler, R. Huber, M. Stöckli, A. Mezzetti, *ACS Catalysis* **2016**, *6*, 6455–6464.
- [13] L. Hintermann, C. Dittmer, *Eur. J. Org. Chem.* **2012**, *2012*, 5573–5584.
- [14] P. Kuzmic, *Anal. Biochem.* **1996**, *237*, 260.
- [15] W. Zuo, D. E. Prokopchuk, A. J. Lough, R. H. Morris, *ACS Catal.* **2016**, *6*, 301–314.
- [16] T. Eixelsberger, J. M. Woodley, B. Nidetzky, R. Kratzer, *Biotechnol. Bioeng.* **2013**, *100*, 2311–2231.
- [17] K. M. J. Brands, J. F. Payack, J. D. Rosen, T. D. Nelson, A. Candelario, M. A. Huffman, M. M. Zhao, J. Li, B. Craig, Z. J. Song, D. M. Tschaen, K. Hansen, P. N. Devine, P. J. Pye, K. Rossen, P. G. Dormer, R. A. Reamer, C. J. Welch, D. J. Mathre, N. N. Tsou, J. M. McNamara, P. J. Reider, *J. Am. Chem. Soc.* **2003**, *125*, 2129–2135.
- [18] a) C. A. Tolman, S. D. Ittel, A. D. English, J. P. Jesson, *J. Am. Chem. Soc.* **1978**, *100*, 4080–4089; b) N. Bampos, L. D. Field, *Inorg. Chem.* **1990**, *29*, 587–588; c) C. Bianchini, M. Peruzzini, A. Polo, A. Vacca, F. Zanobini, *Gazz. Chim. Ital.* **1991**, *121*, 543–549; d) G. Jia, S. D. Drouin, P. G. Jessop, A. J. Lough, R. H. Morris, *Organometallics* **1993**, *12*, 906–916; e) N. Bampos, L. D. Field, B. A. Messerle, *Organometallics* **1993**, *12*, 2529–2535; f) D. G. Gusev, R. Huebener, P. Burger, O. Orama, H. Berke, *J. Am. Chem. Soc.* **1997**, *119*, 3716–3731; g) D. Schott, P. Callaghan, J. Dunne, S. B. Duckett, C. Godard, J. M. Goicoechea, J. N. Harvey, J. P. Lowe, R. J. Mawby, G. Müller, R. N. Perutz, R. Poli, M. K. Whittlesey, *Dalton Trans.* **2004**, 3218–3224; h) R. J. Trovitch, E. Lobkovsky, P. J. Chirik, *Inorg. Chem.* **2006**, *45*, 7252–7260; i) P. Bhattacharya, J. A. Krause, H. Guan, *Organometallics* **2011**, *30*, 4720–4729.
- [19] a) M. Bautista, K. A. Earl, R. H. Morris, A. Sella, *J. Am. Chem. Soc.* **1987**, *109*, 3780–3782; b) M. T. Bautista, K. A. Earl, R. H. Morris, *Inorg. Chem.* **1988**, *27*, 1124–1126; c) M. T. Bautista, E. P. Cappellani, S. D. Drouin, R. H. Morris, C. T. Schweitzer, A. Sella, J. Zubkowski, *J. Am. Chem. Soc.* **1991**, *113*, 4876–4887; d) E. Rocchini, P. Rigo, A. Mezzetti, T. Stephan, R. H. Morris, A. J. Lough, C. E. Forde, T. P. Fong, S. D. Drouin, *J. Chem. Soc., Dalton Trans.* **2000**, 3591–3602; e) R. Langer, G. Leitus, Y. Ben-David, D. Milstein, *Angew. Chem. Int. Ed.* **2011**, *50*, 2120–2124; f) B. Bichler, C. Holzhaecker, B. Stoger, M. Puchberger, L. F. Veiros, K. Kirchner, *Organometallics* **2013**, *32*, 4114–4121; g) F. Bertini, N. Gorgas, B. Stoger, M. Peruzzini, L. F. Veiros, K. Kirchner, L. Gonsalvi, *ACS Catal.* **2016**, *6*, 2889–2893; h) F. Schneck, M. Assmann, M. Balmer, K. Harms, R. Langer, *Organometallics* **2016**; i) S. Elangovan, B. Wendt, C. Topf, S. Bachmann, M. Scalone, A. Spannenberg, H. J. Jiao, W. Baumann, K. Junge, M. Beller, *Adv. Synth. Catal.* **2016**, *358*, 820–825.
- [20] G. Guilera, G. S. McGrady, J. W. Steed, R. P. L. Burchell, P. Sirsch, A. J. Deeming, *New J. Chem.* **2008**, *32*, 1573–1581.
- [21] D. E. Prokopchuk, R. H. Morris, *Organometallics* **2012**, *31*, 7375–7385.

Received: March 31, 2017

Accepted: August 4, 2017

Published online on ■■■ 0000

FULL PAPER



S. A. M. Smith, D. E. Prokopchuk,
R. H. Morris*

1 – 13

Asymmetric Transfer Hydrogenation of Ketones Using New Iron(II) (P-NH-N-P') Catalysts: Changing the Steric and Electronic Properties at Phosphorus P'

